EUROPEAN ORGANIZATION FOR NUCLEAR RESEARCH

Proposal to the ISOLDE and Neutron Time-of-Flight Committee

Measurement of the changes in the mean-square charge radii of aluminium isotopes across $N = 20$

May 12, 2021

Á. Koszorús,[1] M. Athanasakis-Kaklamanakis,[2,3] S. Bara,[2] R. P. de Groote,[4] M. L. Bissell,[5] A.J. Brinson,[6] T. E. Cocolios,[2] K. T. Flanagan,[5,7] S. Franchoo,[8] R. F. Garcia Ruiz,[6] S. Geldhof,[2] J.D. Johnson,[2] J. Karthein,[6] G. Neyens,[2,3] S.M. Udrescu,[6] A R. Vernon,[6] S. G. Wilkins,[6] X. F. Yang,[9]

[1]*Department of Physics, University of Liverpool, Liverpool L69 7ZE, United Kingdom*
[3]*Instituut voor Kern- en Stralingsfysica,KU Leuven, B-3001 Leuven, Belgium*
[2]*Physics Department, CERN, CH-1211 Geneva 23, Switzerland*
[4]*Department of Physics, University of Jyväskylä, PB 35(YFL) FIN-40351 Jyväskylä, Finland*
[5]*School of Physics and Astronomy, The University of Manchester, Manchester M13 9PL, United Kingdom*
[8]*Massachusetts Institute of Technology, Cambridge, MA 02139, USA*
[6]*Photon Science Institute Alan Turing Building, University of Manchester, Manchester M13 9PY, United Kingdom*
[7]*Irène Joliot-Curie Laboratory, IJC/CNRS, 91405 Orsay Cedex, France*
[9]*School of Physics and State Key Laboratory of Nuclear Physics and Technology, Peking University, Beijing 100871, China*

Spokesperson: Á. Koszorús [agota.koszorus@cern.ch]
Contact person: S. Geldhof [sarina.geldhof@kuleuven.be]

CERN-INTC-2021-034 / INTC-P-605
12/05/2021

Abstract: We propose to measure the changes in the mean-square nuclear charge radii of exotic aluminium ($Z = 13$) isotopes with the Collinear Resonance Ionization Spectroscopy (CRIS) method. Using the CRIS technique the charge radii across the neutron shell closure at $N = 20$ can be obtained by performing measurements on ^{33,34}Al, with $N = 20$ and $N = 21$ respectively. These results will provide the first insight into the evolution of the nuclear charge distribution across $N = 20$ in the vicinity of the island inversion.

Requested shifts: 15 shifts of radioactive beam and 1 shift of stable beam

1 Introduction

The aluminium ($Z = 13$) isotopes $^{33-34}$Al are located at the edge of the island of inversion around $N = 20$ [1, 2] as depicted in Fig. 1. This name refers to the region on the nuclear chart where the ground-state structure is dominated by particle-hole (p-h) excitations of neutrons across the reduced $N = 20$ shell gap, leading to unexpected ground-state deformation. These so-called 'intruder' configurations can become the ground state, as their energy lowers due to enhanced quadrupole and pairing correlations [3]. When the ground state wave function of an isotope is dominated or strongly mixed with intruder configurations the isotope is said to be within the island of inversion. Experimental signatures of the onset of deformation in this region have initially come from measured binding energies across $N = 20$ and charge radii up to $N = 20$ in Na [4, 5]. The presence of deformation, despite the magic $N = 20$ shell closure, also prevails in Mg. This has been identified in the measured energy of the 2_1^+ states of ^{32,34}Mg [6, 7], the appearance of shape coexisting 0^+ states in ^{32}Mg [8], and later in the charge radii and moments of ^{31,32}Mg [9, 10] and the binding energies [11]. In the latter, the smallest observed shell gap was reported for any nuclide with a canonical magic number. In contrast, the next even-Z Si ($Z = 14$) isotopes maintain a spherical ground state [12]. Aluminium is thus wedged between the deformed Mg ($Z = 12$) and the spherical Si ($Z = 14$) isotopes. The structure of the ^{33,34}Al isotopes has been inferred from their measured g-factors and nuclear quadruple moments: the isotopes have a mixed wavefunction, composed of normal and intruder configurations, and thus form a gradual transition into the island of inversion below $Z = 13$ [1, 2, 13, 14].

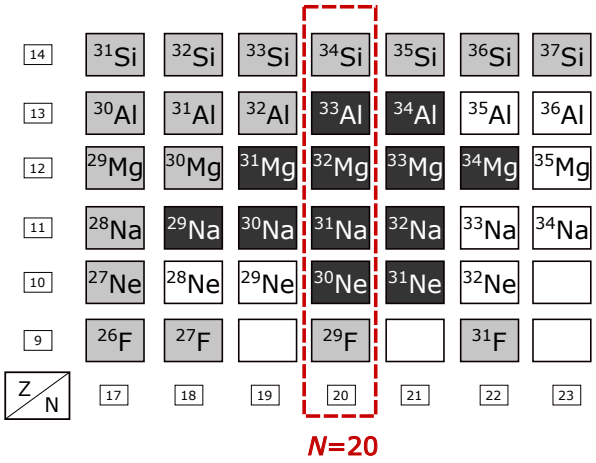

Figure 1: The region of the island of inversion in the vicinity of $N = 20$. The white rectangles represent isotopes for which the configurations are unknown, the gray have normal ground-state configurations without neutron excitations across $N = 20$. The dark isotopes have a ground-state structure which is dominated by (or heavily mixed with) 2p-2h configurations.

The two-neutron separation energies extracted from precise mass measurements are known in and around the island of inversion, as presented in Fig. 2(a), and play an important

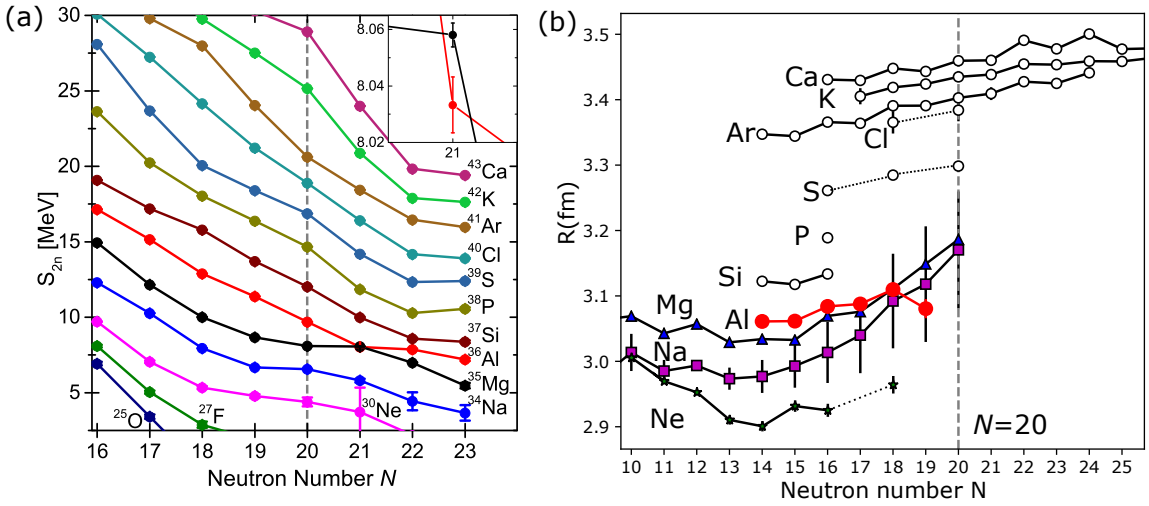

Figure 2: (a) The measured S_{2n} in the region. (b) The measured charge radii in the island of inversion and across $N = 20$. Figure (a) is taken from [15].

role in understanding the evolution of the shell structure in the region [4, 11, 15, 16, 17]. Interestingly, at $N = 21$ the only crossover in the S_{2n} trends was detected on the nuclear chart between the ^{34}Al and ^{33}Mg isotopes [16], which is highlighted in the inset of Fig. 2 (a). In contrast, there are no measurements of the charge radii above $N = 20$, as shown in Fig. 2(b). Nevertheless, the available results for Na and Mg stretching up to $N = 20$ have revealed a striking correlation between the trend in the charge radii and the occupation of the neutron orbitals [5, 9], demonstrating the sensitivity of this property to the details of the nuclear structure in the island of inversion, as will be discussed below.

2 Physics Motivation

The Al isotopes are well-positioned to investigate the evolution of the charge radii across the $N = 20$ neutron shell gap in the island of inversion. Charge radii are considered to be sensitive probes of changes in the nuclear structure such as deformation [18] and shell closures [19]. In general, the stabilizing effect of a magic shell results in a significant change in the nuclear charge distribution before and after the magic number. The available experimental data across $N = 20$ so far is limited to 3 isotopic chains, Ar ($Z = 18$) [20, 21], K ($Z = 19$) [22, 23], and Ca ($Z = 20$) [24]. In all of these $N = 20$ occurs close to stability. Interestingly, from these data no clear signature of a shell closure at $N = 20$ is detected in the charge radii. This finding has been attributed to the cancellation of the monopole and quadrupole polarization of the proton core as neutrons are added [20]. Laser spectroscopy experiments on more exotic isotopes below Ar with $N = 20$ could not be performed thus far, as the production and extraction of these isotopes at radioactive ion beam facilities is very challenging due to their chemical properties. In addition, laser spectroscopy of Cl ($Z = 17$), S ($Z = 16$) and P ($Z = 15$) is not trivial with current laser systems and measurements methods. Therefore, going south from Ar, the first element which can be studied is the Al chain.

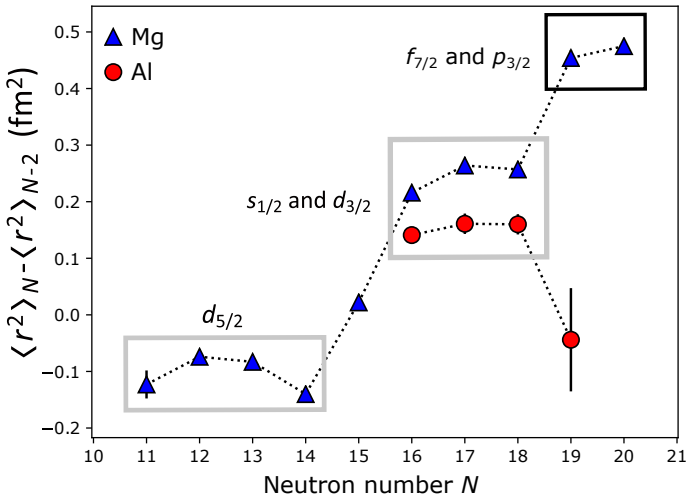

Figure 3: The differential mean-square charge radii are sensitive to the structural changes in the island of inversion, in particular to the filling of specific neutron orbitals and excitation across $N = 20$. While a similar trend is observed in between $N = 16$ and $N = 18$ in the Al and Mg chain, a different behavior is present approaching N=20.

Previously, the neutron-rich Al isotopes have been studied at ISOLDE using collinear laser spectroscopy, where measurements up to ^{32}Al (N=19) were performed [25]. The extracted charge radii of Al are presented in red in Fig. 2(b), together with the neighbouring isotopic chains. The charge radii of Mg and Na have been measured up to $N = 20$ [5, 9], and a proposal to study the Mg isotopes beyond $N = 20$ has been accepted for the new MIRACLS experiment [26]. The charge radius at ^{32}Al ($N = 19$), unexpectedly deviates from the trend approaching $N = 20$. Though the uncertainty on this value is large, a 2σ deviation is observed from the gradually increasing sizes in the region. This could result from reduced correlations at the $N = 20$ closed shell in the Al isotopes, as pointed out in [25]. On the other hand, both electromagnetic moments of ^{33}Al ($N = 20$) and ^{34}Al ($N = 21$) suggest that cross-shell excitations play an important role in their structure [1, 2, 13]. The authors of Ref. [25] therefore pointed out that a more precise measurement of the charge radius of ^{32}Al is required to derive a firm conclusion.

In addition, the changes in the mean-square charge radii are good indicators of the structural changes in the island of inversion [5, 9]. In Fig. 3, the differential charge radii of Al and Mg are compared. This quantity is essentially the increase in the mean-square charge radii when two neutrons are added. Indeed, a clear correlation is present between the occupation of particular neutron orbitals and the proton distribution [9]. Furthermore, in the case of Mg a significant increase is observed for the isotopes in the island of inversion (^{31}Mg and ^{32}Mg). It is apparent that the measured charge radius of ^{32}Al deviates from the trend of the Mg isotopes. We thus propose to re-measure the nuclear charge radius of ^{32}Al and extend the measurements across $N = 20$, using the

more sensitive collinear resonance ionization spectroscopy method. The charge radii of ^{33,34}Al will not only shed further light on the structure change when crossing $N = 20$, but will also allow us to observe the odd-even staggering at $N = 20$. This quantity has proven to be a sensitive probe for the details of the nuclear force and to detect shell effects [18, 24, 27, 28, 29].

From the theoretical point of view, configuration interaction calculations (e.g. large-scale shell model) and mean-field methods were most often employed to test our understanding of the island of inversion [30, 31, 32, 33, 34]. Until recently, *ab initio* coupled cluster (CC) calculations could only be performed in the vicinity of magic numbers of even-Z isotopes [35, 36]. However recent advances allowed for the calculation of the properties of isotopes across neutron shells and odd-Z systems as well [28, 37]. Thanks to this progress, the region of the island of inversion can now be investigated using these state-of-the-art potentials and computational methods. In Ref. [38], of particular interest was the trend of the charge radii across $N = 20$, to investigate the impact (or lack thereof) of this magic number and the onset of deformation. However, the predictions of CC calculations beyond $N = 20$ could not be tested due to the lack of experimental data. Furthermore, calculations employing the Valence Space In-Medium Similarity Renormalization Group (VS-IMSRG) method are also available for the region we propose to study [39]. This method successfully predicted the odd-even staggering of the nuclear charge radius and binding energies in the Cu isotopes [27]. Furthermore, VS-IMSRG calculations are readily available for the Al chain [25]. These are thus perfectly suited to examine the trend of the charge radii across $N = 20$. The comparison of new experimental data to predictions of the state-of-the-art theoretical calculations will be a stringent test of the advances on this front.

In summary, we propose to provide the first measurement of the charge radii across N=20 in the vicinity of Mg, probing the evolution of the nuclear charge distribution and the effect of the reduced shell gap at the edge of the island of inversion.

3 Experimental details

The proposed isotopes will be studied using the Collinear Resonance Ionization Spectroscopy setup (CRIS). Previously, laser spectroscopy on Al isotopes has been performed using the optically detected collinear laser spectroscopy method at both ISOLDE [25] and the IGISOL facility [40]. In addition, the first proof-of-principle experiment of the CRIS technique was performed on ^{27}Al with an efficiency of 1 in 500 at the IGISOL [41]. As a result, there is a solid understanding of the efficiency of different stages of the experiment.

The ions will be cooled and bunched in the ISCOOL device, having better than 50% transmission efficiency at the masses of interest. These bunches will be guided to the CRIS beamline where neutralization will take place in the K- or Na- filled charge-exchange cell (CEC). Both of these neutralisation efficiencies were tested in the previous COLLAPS and

IGISOL experiments. The expected population of different low-lying states are between 20% and 50% [42]. The remaining ions can be deflected from the beam using an electrostatic deflector after the CEC. Next, resonant excitation and subsequent non-resonant ionization will take place in the interaction region of the CRIS beamline. Here the atom beam and the laser light will be overlapped in the collinear geometry. The wavelength of the laser used for the first excitation will be continuously changed, probing all possible hyperfine transitions. A high-power ionization laser with sufficient energy will ionize the excited atoms. Finally, these ions will then be deflected towards a MagneToF particle detector. The hyperfine structure is reconstructed by plotting the frequency of the scanning laser and the corresponding ion count rate.
The isotope shift $\nu^{AA'}$ is calculated as the difference between the centroid of the fitted hyperfine structure of two isotopes, with one being the reference. The hyperfine structure of the reference isotope has to be measured in regular time intervals to account for the long-term drift in the voltage and wavelength readout [43]. The changes of the mean-square charge radii $\delta\langle r^2\rangle^{AA'}$ are calculated as:

$$\delta\langle r^2\rangle^{AA'} = \frac{1}{F}\Big(\nu^{AA'} - (K_{\mathrm{NMS}} + K_{\mathrm{SMS}})\frac{m_A - m_{A'}}{m_A m_{A'}}\Big), \tag{1}$$

where m_A, $m_{A'}$ are the masses of the isotopes A and A', F is the atomic field shift, K_{NMS} and K_{SMS} are the normal and specific mass shifts. The latter parameters are properties of the atomic transitions, and are obtained from atomic physics calculations.

3.1 Laser ionization schemes

Suggested ionization schemes with reasonable sensitivity to the nuclear properties are presented in Fig. 4. All the laser wavelengths presented in this figure can readily be produced with the current laser systems in the CRIS laser laboratory. The transition from the $J = 3/2$ state at 395 nm was used in the recent experiments at COLLAPS and IGISOL [25, 40]. Ionizing the atom after exciting with this transition however requires the use of a 355 nm high-energy laser, which could lead to high non-resonant ionization rates of isobaric contaminants (if present), and thus may result in high background rates. The other transitions would therefore be more suitable. In addition, it would be favorable to use a transition from the atomic ground state with $J = 1/2$, as this reduces the number of hyperfine components to be scanned over. This is advantageous for isotopes with low production rates, since it reduces the time required to reach sufficient statistics. Note, that a long-lived $I^\pi = 1^+$ isomer has been identified in ^{34}Al with 26 ms half life. However, at ISOLDE this isomer was not present in the ^{34}Al beam, and has only been produced by in-trap decay of ^{34}Mg [17]. The measurement of this isomeric state is therefore not part of this proposal.

4 Yield and shift estimates

The summary of the beam request and estimated number of shifts required for the measurements is presented in Table 1. The yields were taken from the ISOLDE online yields

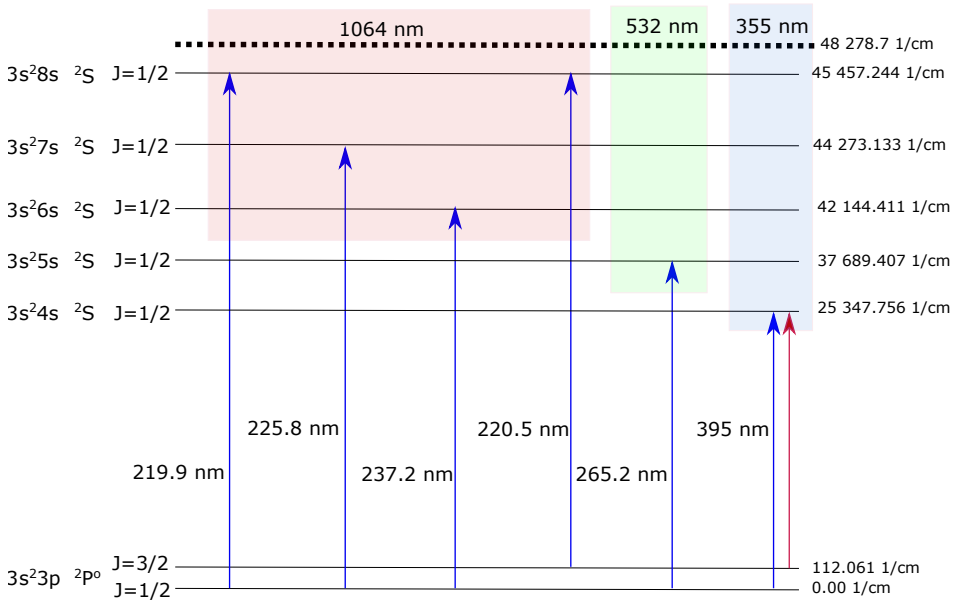

Figure 4: Possible laser ionization schemes for the Al atoms. The first resonant laser excitation is presented by arrows and the subsequent non-resonant ionization step is shown as a shaded area. The red arrow indicates the transition previously used at COLLAPS and IGISOL.

database [44].
The shifts requested for the re-measurement of $^{27-31}$Al are necessary to enable the voltage calibration and overlap of the dataset with previous results using the COLLAPS technique. This will also allow for the investigation of any systematic deviations between the two measurements with different laser spectroscopy techniques [43].

Table 1: Production yields and requested shifts for the measurement of neutron-rich aluminium isotopes [44].

Isotope	Half life	Predicted yield	Shifts
^{27}Al	stable		0.5
$^{28-31}$Al	>500 ms	$2 > 10^5$	2
^{32}Al	33 ms	not listed	1.5
^{33}Al	41.7 ms	$4.9{\cdot}10^2$	2
^{34}Al	56 ms	$>1{\cdot}10^1$	9
Beam tuning			1
RILIS			yes
		Total	16

For the extraction of precise isotope shifts, frequent reference measurements are crucial. Based on previous successful experiments, close to 1/4 of the shifts are spent on these measurements. This time is taken into account in the shift request. Given that in the light isotopes such as Al, the atomic transitions are less sensitive to the changes in

the mean-square charge radius, more precise isotope shift measurements are required resulting in longer measurement times as compared to other CRIS measurements performed in the past.

The production yields of ^{33,34}Al are less than 500 ions/s, which makes precision measurement of their isotope shifts challenging. This is reflected in the beamtime request, where we request 2 and 9 shifts for ^{33,34}Al respectively. Previously, CRIS has been successfully performed on isotopes produced with such low rates [27, 28, 45], with the 20 ion/s marking the most challenging case so far.

Summary of requested shifts: 15 shifts are requested using a UC_x target and 1 shift with stable beam.

References

[1] H. Heylen, M. De Rydt, G. Neyens, M. L. Bissell, L. Caceres, R. Chevrier, J. M. Daugas, Y. Ichikawa, Y. Ishibashi, O. Kamalou, T. J. Mertzimekis, P. Morel, J. Papuga, A. Poves, M. M. Rajabali, C. Stödel, J. C. Thomas, H. Ueno, Y. Utsuno, N. Yoshida, and A. Yoshimi. High-precision quadrupole moment reveals significant intruder component in $^{33}_{13}\mathrm{Al}_{20}$ ground state. *Phys. Rev. C*, 94:034312, Sep 2016.

[2] P. Himpe, G. Neyens, D.L. Balabanski, G. Bélier, J.M. Daugas, F. de Oliveira Santos, M. De Rydt, K.T. Flanagan, I. Matea, P. Morel, Yu.E. Penionzhkevich, L. Perrot, N.A. Smirnova, C. Stodel, J.C. Thomas, N. Vermeulen, D.T. Yordanov, Y. Utsuno, and T. Otsuka. g factor of the exotic $N = 21$ isotope ^{34}Al: probing the N=20 and N=28 shell gaps at the border of the "island of inversion". *Physics Letters B*, 658(5):203–208, 2008.

[3] Kris Heyde and John L. Wood. Shape coexistence in atomic nuclei. *Rev. Mod. Phys.*, 83:1467–1521, Nov 2011.

[4] C. Thibault, R. Klapisch, C. Rigaud, A. M. Poskanzer, R. Prieels, L. Lessard, and W. Reisdorf. Direct measurement of the masses of ^{11}Li and $^{26-32}$Na with an on-line mass spectrometer. *Phys. Rev. C*, 12:644–657, Aug 1975.

[5] G. Huber, F. Touchard, S. Büttgenbach, C. Thibault, R. Klapisch, H. T. Duong, S. Liberman, J. Pinard, J. L. Vialle, P. Juncar, and P. Jacquinot. Spins, magnetic moments, and isotope shifts of $^{21-31}$Na by high resolution laser spectroscopy of the atomic D_1 line. *Phys. Rev. C*, 18:2342–2354, Nov 1978.

[6] C. Détraz, D. Guillemaud, G. Huber, R. Klapisch, M. Langevin, F. Naulin, C. Thibault, L. C. Carraz, and F. Touchard. Beta decay of $^{27-32}$Na and their descendants. *Phys. Rev. C*, 19:164–176, Jan 1979.

[7] J. A. Church, C. M. Campbell, D.-C. Dinca, J. Enders, A. Gade, T. Glasmacher, Z. Hu, R. V. F. Janssens, W. F. Mueller, H. Olliver, B. C. Perry, L. A. Riley, and K. L. Yurkewicz. Measurement of $e2$ transition strengths in ^{32,34}Mg. *Phys. Rev. C*, 72:054320, Nov 2005.

[8] K. Wimmer, T. Kröll, R. Krücken, V. Bildstein, R. Gernhäuser, B. Bastin, N. Bree, J. Diriken, P. Van Duppen, M. Huyse, N. Patronis, P. Vermaelen, D. Voulot, J. Van de Walle, F. Wenander, L. M. Fraile, R. Chapman, B. Hadinia, R. Orlandi, J. F. Smith, R. Lutter, P. G. Thirolf, M. Labiche, A. Blazhev, M. Kalkühler, P. Reiter, M. Seidlitz, N. Warr, A. O. Macchiavelli, H. B. Jeppesen, E. Fiori, G. Georgiev, G. Schrieder, S. Das Gupta, G. Lo Bianco, S. Nardelli, J. Butterworth, J. Johansen, and K. Riisager. Discovery of the shape coexisting 0^+ state in ^{32}Mg by a two neutron transfer reaction. *Phys. Rev. Lett.*, 105:252501, Dec 2010.

[9] D. T. Yordanov, M. L. Bissell, K. Blaum, M. De Rydt, Ch. Geppert, M. Kowalska, J. Krämer, K. Kreim, A. Krieger, P. Lievens, T. Neff, R. Neugart, G. Neyens,

W. Nörtershäuser, R. Sánchez, and P. Vingerhoets. Nuclear charge radii of $^{21-32}$Mg. *Phys. Rev. Lett.*, 108:042504, Jan 2012.

[10] G. Neyens, M. Kowalska, D. Yordanov, K. Blaum, P. Himpe, P. Lievens, S. Mallion, R. Neugart, N. Vermeulen, Y. Utsuno, and T. Otsuka. Measurement of the spin and magnetic moment of ^{31}Mg: Evidence for a strongly deformed intruder ground state. *Phys. Rev. Lett.*, 94:022501, Jan 2005.

[11] A. Chaudhuri, C. Andreoiu, T. Brunner, U. Chowdhury, S. Ettenauer, A. T. Gallant, G. Gwinner, A. A. Kwiatkowski, A. Lennarz, D. Lunney, T. D. Macdonald, B. E. Schultz, M. C. Simon, V. V. Simon, and J. Dilling. Evidence for the extinction of the $N = 20$ neutron-shell closure for ^{32}Mg from direct mass measurements. *Phys. Rev. C*, 88:054317, Nov 2013.

[12] R. W. Ibbotson, T. Glasmacher, B. A. Brown, L. Chen, M. J. Chromik, P. D. Cottle, M. Fauerbach, K. W. Kemper, D. J. Morrissey, H. Scheit, and M. Thoennessen. Quadrupole collectivity in ^{32,34,36,38}Si and the $N = 20$ shell closure. *Phys. Rev. Lett.*, 80:2081–2084, Mar 1998.

[13] P. Himpe, G. Neyens, D.L. Balabanski, G. Bélier, D. Borremans, J.M. Daugas, F. de Oliveira Santos, M. De Rydt, K. Flanagan, G. Georgiev, M. Kowalska, S. Mallion, I. Matea, P. Morel, Yu.E. Penionzhkevich, N.A. Smirnova, C. Stodel, K. Turzó, N. Vermeulen, and D. Yordanov. g factors of ^{31,32,33}Al: Indication for intruder configurations in the ^{33}Al ground state. *Physics Letters B*, 643(5):257–262, 2006.

[14] Z.Y. Xu, H. Heylen, K. Asahi, F. Boulay, J.M. Daugas, R.P. de Groote, W. Gins, O. Kamalou, Á. Koszorús, M. Lykiardopoulou, T.J. Mertzimekis, G. Neyens, H. Nishibata, T. Otsuka, R. Orset, A. Poves, T. Sato, C. Stodel, J.C. Thomas, N. Tsunoda, Y. Utsuno, M. Vandebrouck, and X.F. Yang. Nuclear moments of the low-lying isomeric 1+ state of ^{34}Al: Investigation on the neutron 1p1h excitation across N=20 in the island of inversion. *Physics Letters B*, 782:619–626, 2018.

[15] A. A. Kwiatkowski, C. Andreoiu, J. C. Bale, A. Chaudhuri, U. Chowdhury, S. Malbrunot-Ettenauer, A. T. Gallant, A. Grossheim, G. Gwinner, A. Lennarz, T. D. Macdonald, T. J. M. Rauch, B. E. Schultz, S. Seeraji, M. C. Simon, V. V. Simon, D. Lunney, A. Poves, and J. Dilling. Observation of a crossover of S_{2n} in the island of inversion from precision mass spectrometry. *Phys. Rev. C*, 92:061301, Dec 2015.

[16] A. T. Gallant, M. Alanssari, J. C. Bale, C. Andreoiu, B. R. Barquest, U. Chowdhury, J. Even, A. Finlay, D. Frekers, G. Gwinner, R. Klawitter, B. Kootte, A. A. Kwiatkowski, D. Lascar, K. G. Leach, E. Leistenschneider, A. Lennarz, A. J. Mayer, D. Short, R. Thompson, M. Wieser, D. Lunney, and J. Dilling. Mass determination near $N = 20$ for Al and Na isotopes. *Phys. Rev. C*, 96:024325, Aug 2017.

[17] P. Ascher, N. Althubiti, D. Atanasov, K. Blaum, R. B. Cakirli, S. Grévy, F. Herfurth, S. Kreim, D. Lunney, V. Manea, D. Neidherr, M. Rosenbusch, L. Schweikhard,

A. Welker, F. Wienholtz, R. N. Wolf, and K. Zuber. Mass measurements of neutron-rich isotopes near $N = 20$ by in-trap decay with the isoltrap spectrometer. *Phys. Rev. C*, 100:014304, Jul 2019.

[18] B. A. Marsh, T. Day Goodacre, S. Sels, Y. Tsunoda, B. Andel, A. N. Andreyev, N. A. Althubiti, D. Atanasov, A. E. Barzakh, J. Billowes, K. Blaum, T. E. Cocolios, J. G. Cubiss, J. Dobaczewski, G. J. Farooq-Smith, D. V. Fedorov, V. N. Fedosseev, K. T. Flanagan, L. P. Gaffney, L. Ghys, M. Huyse, S. Kreim, D. Lunney, K. M. Lynch, V. Manea, Y. Martinez Palenzuela, P. L. Molkanov, T. Otsuka, A. Pastore, M. Rosenbusch, R. E. Rossel, S. Rothe, L. Schweikhard, M. D. Seliverstov, P. Spagnoletti, C. Van Beveren, P. Van Duppen, M. Veinhard, E. Verstraelen, A. Welker, K. Wendt, F. Wienholtz, R. N. Wolf, A. Zadvornaya, and K. Zuber. Characterization of the shape-staggering effect in mercury nuclei. *Nature Phys.*, 14(12):1163–1167, 2018.

[19] C. Gorges, L. V. Rodríguez, D. L. Balabanski, M. L. Bissell, K. Blaum, B. Cheal, R. F. Garcia Ruiz, G. Georgiev, W. Gins, H. Heylen, A. Kanellakopoulos, S. Kaufmann, M. Kowalska, V. Lagaki, S. Lechner, B. Maaß, S. Malbrunot-Ettenauer, W. Nazarewicz, R. Neugart, G. Neyens, W. Nörtershäuser, P.-G. Reinhard, S. Sailer, R. Sánchez, S. Schmidt, L. Wehner, C. Wraith, L. Xie, Z. Y. Xu, X. F. Yang, and D. T. Yordanov. Laser spectroscopy of neutron-rich tin isotopes: A discontinuity in charge radii across the $N = 82$ shell closure. *Phys. Rev. Lett.*, 122(19):192502, 2019.

[20] A. Klein, B.A. Brown, U. Georg, M. Keim, P. Lievens, R. Neugart, M. Neuroth, R.E. Silverans, L. Vermeeren, and ISOLDE Collaboration. Moments and mean square charge radii of short-lived argon isotopes. *Nuclear Physics A*, 607(1):1–22, 1996.

[21] K. Blaum, W. Geithner, J. Lassen, P. Lievens, K. Marinova, and R. Neugart. Nuclear moments and charge radii of argon isotopes between the neutron-shell closures N=20 and N=28. *Nuclear Physics A*, 799(1):30–45, 2008.

[22] F. Touchard, P. Guimbal, S. Büttgenbach, R. Klapisch, M. De Saint Simon, J.M. Serre, C. Thibault, H.T. Duong, P. Juncar, S. Liberman, J. Pinard, and J.L. Vialle. Isotope shifts and hyperfine structure of $^{38–47}$K by laser spectroscopy. *Physics Letters B*, 108(3):169 – 171, 1982.

[23] D. M. Rossi, K. Minamisono, H. B. Asberry, G. Bollen, B. A. Brown, K. Cooper, B. Isherwood, P. F. Mantica, A. Miller, D. J. Morrissey, R. Ringle, J. A. Rodriguez, C. A. Ryder, A. Smith, R. Strum, and C. Sumithrarachchi. Charge radii of neutron-deficient ^{36}K and ^{37}K. *Phys. Rev. C*, 92:014305, Jul 2015.

[24] A. J. Miller, K. Minamisono, A. Klose, D. Garand, C. Kujawa, J. D. Lantis, Y. Liu, B. Maaß, P. F. Mantica, W. Nazarewicz, W. Nörtershäuser, S. V. Pineda, P.-G. Reinhard, D. M. Rossi, F. Sommer, C. Sumithrarachchi, A. Teigelhöfer, and J. Watkins. Proton superfluidity and charge radii in proton-rich calcium isotopes. *Nat. Phys.*, 15:432–436, feb 2019.

[25] H. Heylen, C. S. Devlin, W. Gins, M. L. Bissell, K. Blaum, B. Cheal, L. Filippin, R. F. Garcia Ruiz, M. Godefroid, C. Gorges, J. D. Holt, A. Kanellakopoulos, S. Kaufmann, Á. Koszorús, K. König, S. Malbrunot-Ettenauer, T. Miyagi, R. Neugart, G. Neyens, W. Nörtershäuser, R. Sánchez, F. Sommer, L. V. Rodríguez, L. Xie, Z. Y. Xu, X. F. Yang, and D. T. Yordanov. High-resolution laser spectroscopy of $^{27-32}$Al. *Phys. Rev. C*, 103:014318, Jan 2021.

[26] INTC-P-565, MIRACLS at ISOLDE : The Charge Radii of Exotic Magnesium Isotopes. Sep 2020.

[27] RP de Groote, Jon Billowes, Corry L Binnersley, Mark L Bissell, Thomas Elias Cocolios, T Day Goodacre, Gregory James Farooq-Smith, DV Fedorov, Kieran T Flanagan, Serge Franchoo, et al. Measurement and microscopic description of odd-even staggering of charge radii of exotic copper isotopes. *Nature Physics*, 16(6):620–624, 2020.

[28] Á Koszorús, X. F. Yang, W. G. Jiang, S. J. Novario, S. W. Bai, J. Billowes, C. L. Binnersley, M. L. Bissell, T. E. Cocolios, B. S. Cooper, R. P. de Groote, A. Ekström, K. T. Flanagan, C. Forssén, S. Franchoo, R. F. Garcia Ruiz, F. P. Gustafsson, G. Hagen, G. R. Jansen, A. Kanellakopoulos, M. Kortelainen, W. Nazarewicz, G. Neyens, T. Papenbrock, P.-G. Reinhard, C. M. Ricketts, B. K. Sahoo, A. R. Vernon, and S. G. Wilkins. Charge radii of exotic potassium isotopes challenge nuclear theory and the magic character of N = 32. *Nature Physics*, 2021.

[29] G. J. Farooq-Smith, A. R. Vernon, J. Billowes, C. L. Binnersley, M. L. Bissell, T. E. Cocolios, T. Day Goodacre, R. P. de Groote, K. T. Flanagan, S. Franchoo, R. F. Garcia Ruiz, W. Gins, K. M. Lynch, B. A. Marsh, G. Neyens, S. Rothe, H. H. Stroke, S. G. Wilkins, and X. F. Yang. Probing the $_{31}$Ga ground-state properties in the region near $Z = 28$ with high-resolution laser spectroscopy. *Phys. Rev. C*, 96:044324, Oct 2017.

[30] Yutaka Utsuno, Takaharu Otsuka, Takahiro Mizusaki, and Michio Honma. Varying shell gap and deformation in $N \sim 20$ unstable nuclei studied by the monte carlo shell model. *Phys. Rev. C*, 60:054315, Oct 1999.

[31] T. Otsuka, M. Honma, T. Mizusaki, N. Shimizu, and Y. Utsuno. Monte carlo shell model for atomic nuclei. *Progress in Particle and Nuclear Physics*, 47(1):319–400, 2001.

[32] E. Caurier, F. Nowacki, and A. Poves. Merging of the islands of inversion at $N = 20$ and $N = 28$. *Phys. Rev. C*, 90:014302, Jul 2014.

[33] Naofumi Tsunoda, Takaharu Otsuka, Noritaka Shimizu, Morten Hjorth-Jensen, Kazuo Takayanagi, and Toshio Suzuki. Exotic neutron-rich medium-mass nuclei with realistic nuclear forces. *Phys. Rev. C*, 95:021304, Feb 2017.

[34] P.-G. Reinhard, D. J. Dean, W. Nazarewicz, J. Dobaczewski, J. A. Maruhn, and M. R. Strayer. Shape coexistence and the effective nucleon-nucleon interaction. *Phys. Rev. C*, 60:014316, Jun 1999.

[35] R. F. Garcia Ruiz, M. L. Bissell, K. Blaum, A. Ekström, N. Frömmgen, G. Hagen, M. Hammen, K. Hebeler, J. D. Holt, G. R. Jansen, M. Kowalska, K. Kreim, W. Nazarewicz, R. Neugart, G. Neyens, W. Nörtershäuser, T. Papenbrock, J. Papuga, A. Schwenk, J. Simonis, K. A. Wendt, and D. T. Yordanov. Unexpectedly large charge radii of neutron-rich calcium isotopes. *Nature Phys.*, 12(6):594, 2016.

[36] A. Ekström, G. R. Jansen, K. A. Wendt, G. Hagen, T. Papenbrock, B. D. Carlsson, C. Forssén, M. Hjorth-Jensen, P. Navrátil, and W. Nazarewicz. Accurate nuclear radii and binding energies from a chiral interaction. *Phys. Rev. C*, 91:051301, May 2015.

[37] W. G. Jiang, A. Ekström, C. Forssén, G. Hagen, G. R. Jansen, and T. Papenbrock. Accurate bulk properties of nuclei from $A = 2$ to ∞ from potentials with Δ isobars. *Phys. Rev. C*, 102:054301, Nov 2020.

[38] S. J. Novario, G. Hagen, G. R. Jansen, and T. Papenbrock. Charge radii of exotic neon and magnesium isotopes. *Phys. Rev. C*, 102:051303, Nov 2020.

[39] T. Miyagi, S. R. Stroberg, J. D. Holt, and N. Shimizu. Ab initio multishell valence-space hamiltonians and the island of inversion. *Phys. Rev. C*, 102:034320, Sep 2020.

[40] I237. Precise measurement of isomeric and ground state charge radii in the self-conjugate ^{26}Al nucleus. IGISOL 2021.

[41] K.T. Flanagan. Sizes and moments of short-lived nuclear states by laser spectroscopy. *PhD Thesis*, 2004.

[42] A.R. Vernon, J. Billowes, C.L. Binnersley, M.L. Bissell, T.E. Cocolios, G.J. Farooq-Smith, K.T. Flanagan, R.F. Garcia Ruiz, W. Gins, R.P. de Groote, Á. Koszorús, K.M. Lynch, G. Neyens, C.M. Ricketts, K.D.A. Wendt, S.G. Wilkins, and X.F. Yang. Simulation of the relative atomic populations of elements $1 \leq Z \leq 89$ following charge exchange tested with collinear resonance ionization spectroscopy of indium. *Spectrochimica Acta Part B: Atomic Spectroscopy*, 153:61 – 83, 2019.

[43] Á. Koszorús, J. Billowes, C.L. Binnersley, M.L. Bissell, T.E. Cocolios, B.S. Cooper, R.P. de Groote, G.J. Farooq-Smith, V.N. Fedosseev, K.T. Flanagan, S. Franchoo, R.F. Garcia Ruiz, W. Gins, K.M. Lynch, G. Neyens, F.P. Gustafsson, C. Ricketts, H.H. Stroke, A. Vernon, S.G. Wilkins, and X.F. Yang. Resonance ionization schemes for high resolution and high efficiency studies of exotic nuclei at the cris experiment. *Nuclear Instruments and Methods in Physics Research Section B: Beam Interactions with Materials and Atoms*, 463:398 – 402, 2020.

[44] ISOLDE yields database. https://isoyields2.web.cern.ch/YieldBasic.aspx?Z=13. Accessed: 2021-05-04.

[45] Ronald Fernando Garcia Ruiz. Laser spectroscopy of neutron-deficient Sn isotopes. Technical report, CERN, Geneva, Jan 2016.

Appendix

DESCRIPTION OF THE PROPOSED EXPERIMENT

The experimental setup comprises: (*name the fixed-ISOLDE installations, as well as flexible elements of the experiment*)

Part of the	Availability	Design and manufacturing
CRIS experiment	☒ Existing	☒ To be used without any modification

HAZARDS GENERATED BY THE EXPERIMENT (if using fixed installation:) Hazards named in the document relevant for the fixed CRIS installation.